Broadband Conductor Backed-CPW With Substrate-Integrated Coaxial Line to SIW Transition for C-Band

Anil Kumar Nayak, *Student Member, IEEE*, Igor M. Filanovsky, *Life Senior Member, IEEE*, Kambiz Moez, *Senior Member, IEEE*, and Amalendu Patnaik, *Senior Member, IEEE*

***Abstract*—This brief describes a transition from conductor-backed-coplanar waveguide (CB-CPW) with substrate-integrated coaxial line (SICL) to substrate integrated waveguide (SIW). The transition is designed for the C-band frequency range. The CB-CPW slot lines play the main role in widening the bandwidth. These CPW slot lines are providing excitation of both even and odd mode waves in SIW, which improves the impedance bandwidth. Using the proposed concept, the measured single-mode fractional impedance bandwidth of 63.34%, the minimum insertion loss of 0.16 dB, and the overall loss below 25% are achieved. The simulated results are found to be in good agreement with the experimental ones obtained for the prototype developed in the laboratory.**

***Index Terms*—Broadband, conductor backed-CPW, C-band, substrate-integrated coaxial line (SICL), substrate integrated waveguide (SIW).**

I. Introduction

TRANSMISSION lines (TLs) and waveguides have been widely used to transmit microwave signals from one device to another. While TLs offer lower loss at lower frequency, transmission from zero frequency (DC), easy integration with printed circuit board (PCB) components, the waveguides offer lower loss at higher frequencies, higher quality factor, a wider bandwidth, and less interference [1], [2]. Over the time, the structure of the transmission line and waveguides both have changed from 3D structures such as coaxial lines and rectangular/circular waveguides to more economical planar structures like microstrip lines or strip lines and substrate integrated waveguides (SIW) [3], [4], respectively. Most recently, substrate integrated coaxial lines (SICLs) have been introduced as a 2.5 D implementation of coaxial cable offering superior performance to other planar transmission lines while maintaining its planar structure for reduced cost. Although SICL is a shielded construction, transverse-electromagnetic (TEM) mode can propagate within it from zero frequency over a wide spectrum of single-mode operation and is non-dispersive [5]. To achieve tightly integrated high-speed parallel data transmission with little crosstalk and phase distortion, multichannel SICL arrays have been utilized.

The challenge is now to design a transition between planar TL structures and SICL/SIW with a low insertion loss (IL) and a large bandwidth. Attempts to excite SIW employing different types of transitions from coaxial line have been reported [6]–[13]. In [6], an X-band broadband transition between coaxial line and SIW has been designed and tested, with a BW of 30% and insertion loss (IL) of 1.2 dB. The main objective of that work was to get impedance matching for a thin substrate. Similarly, the transition from SMA connector to SIW at X and Ku frequency bands has been proposed in [7], and the fractional BW (FBW) of 38.65% and IL of 0.5 dB have been obtained. The robustness and mass-production fabrication of a broadband transition between coaxial line to half-mode SIW has been described in [8]. Yet, an absolute BW (ABW) of 6 GHz with return loss (RL) above 20 dB has been obtained at the end. Recently, some similar types of transitions using SIW, like coplanar waveguide (CPW) to empty SICL [9], coaxial to empty SIW [10], coaxial array to SIW [11], microstrip to empty SICL [12], and coaxial to air-field SIW (AFSIW) [13] have been reported. Some other transitions to SIW deserve to be mentioned. They include coaxial line to SIW [14], CBCPW to SIW [15], waveguide (WG) to SIW [16], and SIW to air-filled rectangular WG to SIW [17] transitions. This long list stresses the importance of transition and their applications.

This brief aims to improve the transition characteristics (the single-mode bandwidth) from CB-CPW with substrate integrated coaxial line to SIW for the C-band application. The structure was planned as the coaxial line to SIW transition at the 4-8 GHz frequency range, and it was decided to use CB-CPW in the design. The CPW slot lines in SIW may provide in SIW both even and odd mode waves, also called the common-mode and differential mode, respectively. As a result, the impedance matching is found better than that in case of

Manuscript received February 7, 2022; accepted March 8, 2022. Date of publication March 16, 2022; date of current version May 3, 2022. This brief was recommended by Associate Editor V. Paliouras. *(Corresponding author: Kambiz Moez.)*

Anil Kumar Nayak is with the Department of Electronics and Communication Engineering, Indian Institute of Technology Roorkee, Roorkee 247667, India, and also with the Department of Electrical and Computer Engineering, University of Alberta, Edmonton, AB T6G 1H9, Canada (e-mail: anayak@ieee.org).

Igor M. Filanovsky and Kambiz Moez are with the Department of Electrical and Computer Engineering, University of Alberta, Edmonton, AB T6G 1H9, Canada (e-mail: ifilanov@ualberta.ca; kambiz@ualberta.ca).

Amalendu Patnaik is with the Department of Electronics and Communication Engineering, Indian Institute of Technology Roorkee, Roorkee 247667, India (e-mail: apatnaik@ieee.org).

Color versions of one or more figures in this article are available at https://doi.org/10.1109/TCSII.2022.3160075.

Digital Object Identifier 10.1109/TCSII.2022.3160075

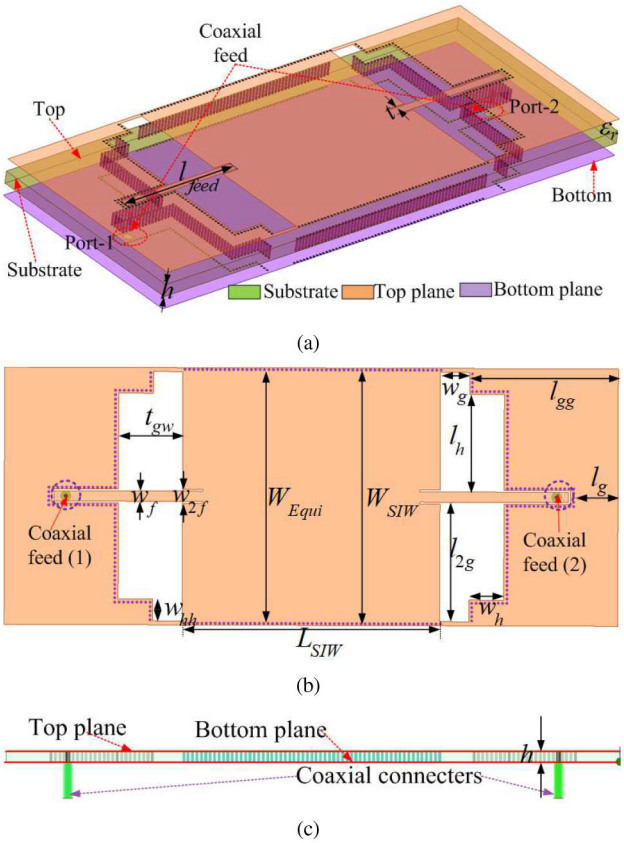

Fig. 1. The proposed transition: (a) Stereoscopic view, (b) Top view, (c) Cross-sectional view.

the simple microstrip line transition between coaxial line and SIW. The transition was fabricated and tested in the laboratory using a vector network analyzer (VNA). The simulated and measured results are in a good agreement.

II. Design and Working Principle of the Transition

Fig. 1 shows the stereoscopic (a), top (b), and cross-sectional (c) views of two back-to-back proposed transitions (the usual practice in the measurements of transition characteristics). The SIW L_{SIW}, W_{SIW} is limited by the metallized vias having the diameter d and the pitch P. The coaxial feed C (Fig. 2) is connected to SIW via microstrip line. Yet, part of this line which is close to the feed contact is separated by a slot from the rest of conductive surface, so it becomes a coplanar waveguide (CPW). In addition, this end is encircled by vias as well, and its properties become very close to that of substrate-integrated coaxial line (SICL). We call this arrangement CPW with SICL properties. The end of this microstrip line entering SIW is also separated from the SIW body by two slots, so it also becomes a CPW, and behaves as two slot lines if one considers that the excitation current can have different directions on the opposite sides of this microstrip. As a result, this CPW may provide even and odd modes of SIW excitation, i.e., provides a wider transition bandwidth. The structure dimensions are $d = 0.35$, $P = 0.6$ (see Fig. 2), $l_{feed} = 20.2$, $w_f = 1.4$, $W_{2f} = 1.9$, $l_g = 6.05$, $l_{gg} = 20.2$, $l_h = 13.3$, $l_{2g} = 16.08$,

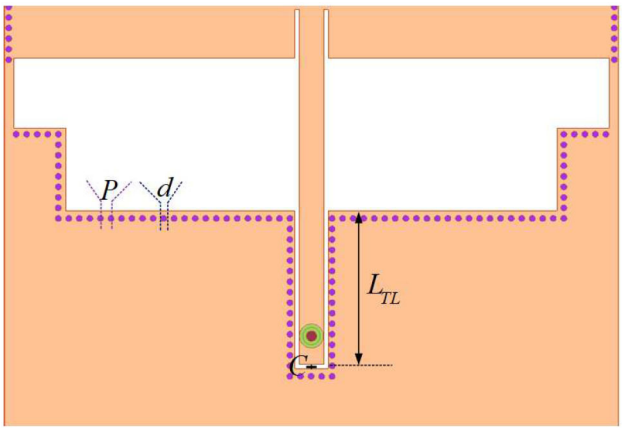

Fig. 2. Position of coaxial feed C.

$w_g = 4$, $t = 0.25$, $w_h = 4.7$, $L_{SIW} = 31$, $W_{SIW} = 34.5$, $W_{hh} = 2.95$, $W_{Equi} = 34.27$, $L_{TL} = 8.48$, $h = 1.524$; unit: millimeters.

The structure was implemented with the Rogers RO4232 material ($\varepsilon_r = 3.2$, $tan\delta = 0.0018$, and $h = 1.524$ mm). The main SIW dimensions, namely, the cut-off frequency f_c, the vias diameter d, and the pitch P, are calculated from the equations [3], [4] used in SIW design as follows:

$$f_c = \frac{c}{2W_{SIW}\sqrt{\varepsilon_r}}; \lambda_g = \frac{\lambda_0}{\sqrt{\varepsilon_r}}; d \le \frac{\lambda_g}{5}; P \le 2d \quad (1)$$

$$W_{Equi} = W_{SIW} - 1.08\frac{d^2}{P} + 0.1\frac{d^2}{W_{SIW}} \quad (2)$$

where λ_g, is the guided wavelength at the center frequency, λ_0 is the wavelength in the free space or air, and ε_r is the relative dielectric constant of the substrate, c is the speed of light. The significant parameter of the transition structure is the impedance matching of the feed and the waveguide. In this design, the width of slot t plays the primary role in providing impedance matching because of this slot the microstrip line behaves like a parallel plate capacitor and it helps to achieve better impedance matching. Finally, the characteristic impedance (Z_0) of the CB-CPW with coaxial feed is nearly equal to 50 Ohm at $t = 0.25$ mm. These dimensions were established by simulations, and the results are discussed in the next section. All simulations were carried out using electromagnetic software HFSS version 2020R2.

To obtain good impedance matching and reduce the losses, the parametric analysis is used in this design. In addition to t, the distance t_{gw} is also a crucial parameter for improving the BW and reducing the IL, as shown in Fig. 3. As t_{gw} varies from 7.7 to 9.7 mm with a step of 0.5 mm, it can be observed that S_{11} is slightly touching the -12 dB line at $t_{gw} = 7.7$ mm. RL goes above 12 dB when the t_{gw} value varies from 7.7 to 8.2 mm. Meanwhile, the IL goes down by 3 dB for the entire passband. Similar results were observed when t_{gw} became 9.7 mm and 9.2 mm. However, the RL and IL are obtained better at $t_{gw} = 8.7$ mm in the whole passband (4-8 GHz). In the end, the value of $t_{gw} = 8.7$ mm is fixed for the transition structure. The electric field and the surface current distributions are calculated at mid-frequency

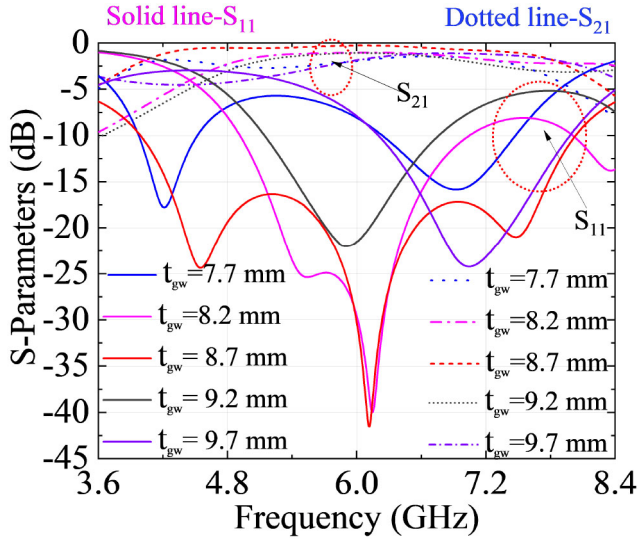

Fig. 3. Simulated S-parameters with different values of t_{gw}.

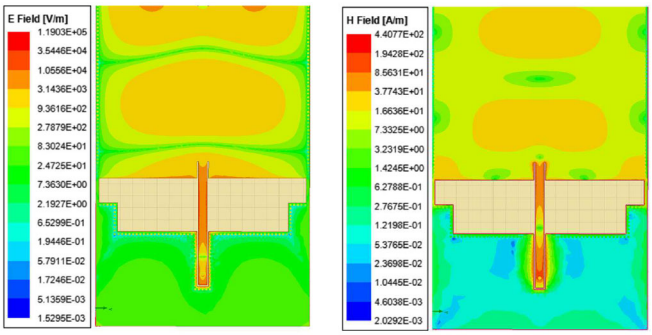

(a) (b)

Fig. 4. Electric and magnetic field pattern in the transition (at 6 GHz).

of the band (6 GHz). These are shown in Fig. 4(a) and (b), respectively.

III. Experimental Validation

Fig. 5 shows the top and bottom views of the laboratory prototype of the transition. All the transition characteristics are measured using the vector network analyzer (VNA model No: N5247A), which can operate in 10 MHz to 67 GHz frequency range. Moreover, the electronics calibration (Ecal) method has been used to do for the experimental validation. The measurements are set up with back-to-back transitions, as shown in Fig. 6. The simulated and measured values of S-parameters are presented in Fig. 7 (a). The measured $|S_{11}|$ (RL) is above 12 dB at the 4.24-8.04 GHz frequency range whereas the simulated RL greater than 12 dB is found from 3.98 GHz to 8.04 GHz frequency range. On the other hand, the minimum simulated and measured $|S_{21}|$ (IL) is obtained below 0.26 and 0.16 ± 0.1 dB, respectively, whereas the maximum IL is found 1.4 and 1.08 ± 0.5 dB for both simulated and measured values. The measured maximum impedance BW of 3.8 GHz (63.34%) has been obtained.The total loss is also calculated and measured, as shown in Fig. 7 (b). The simulated values of the total loss are less than 20% in the frequency range 4.2-7.46 GHz.

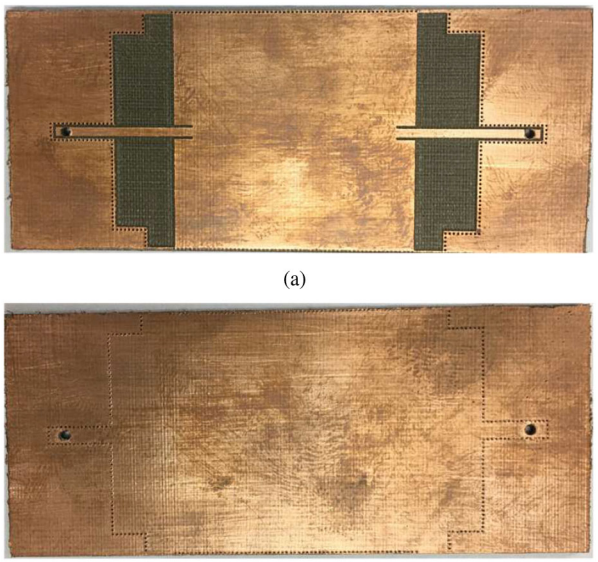

(a)

(b)

Fig. 5. Fabricated prototype of the transition (a) Top view (b) Bottom view.

Fig. 6. The back-to-back transitions with VNA.

A very similar result is obtained using the experimentation, where the total loss is below 25% in the frequency range of 4.6-8.16 GHz. A probable reason for a slight mismatch is the copper paste's connector loss and manual filling of the vias. The power losses in the copper paste filling of the vias in the structure can be noticed by the fact that notches are observed in the experimental phase of S_{21} (Fig. 7 (c)). Yet, the measured results are, on average, in a good agreement with the simulated ones.

To cross verify the generalization of the results obtained, we simulated, fabricated, and measured two additional SIW transitions with different values of L_{SIW}, namely, 36 and 44 mm,

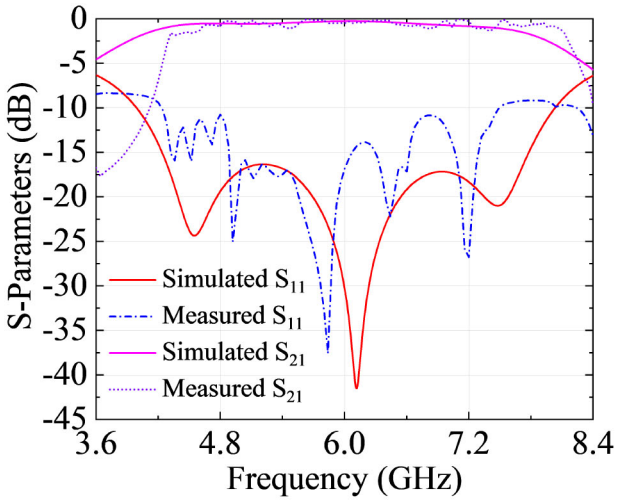

(a)

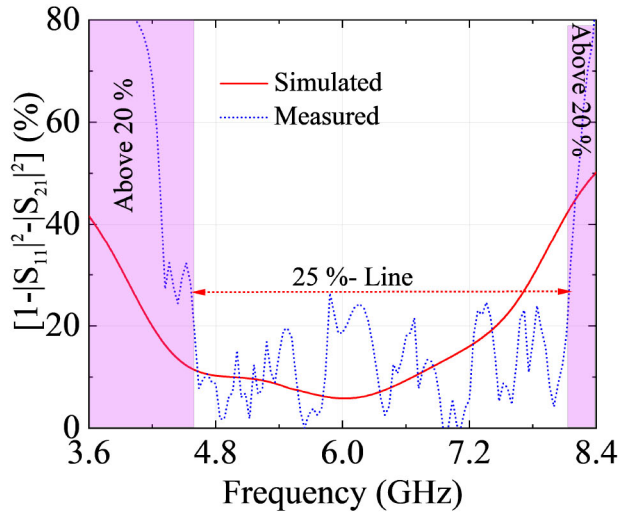

(b)

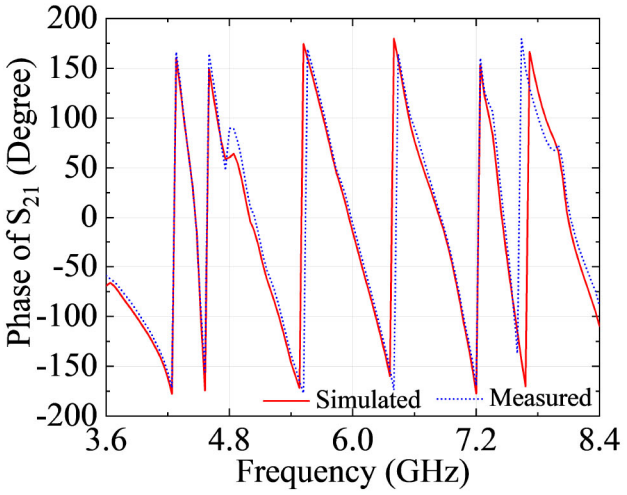

(c)

Fig. 7. Simulated and measured results: (a) $|S_{11}|$ and $|S_{21}|$, (b) Total loss, and (c) Phase of S_{21}.

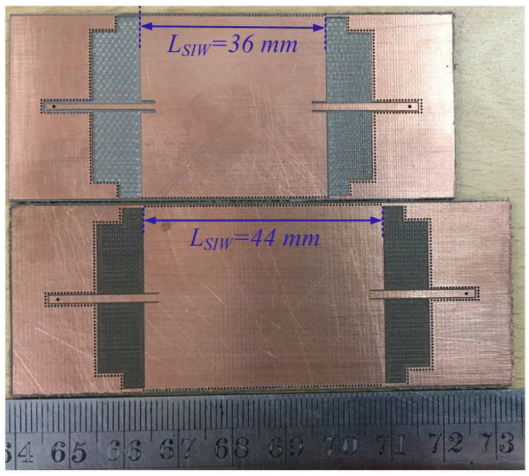

(a)

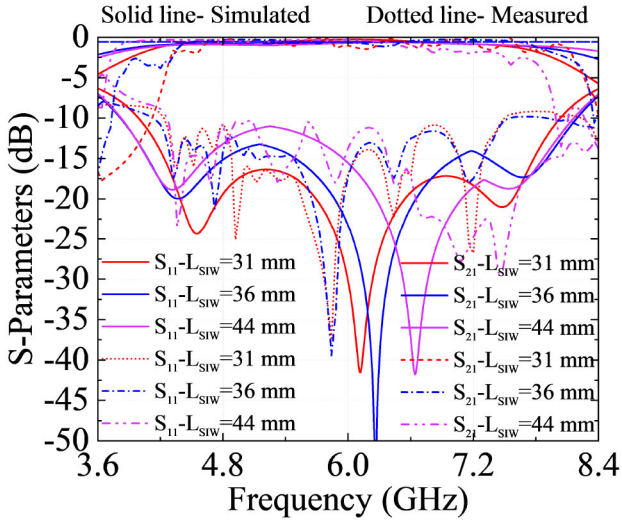

(b)

Fig. 8. Different values of L_{SIW}: (a) Fabrication prototype of transition at L_{SIW} = 36 and 44 mm (b) Simulated and measured $|S_{11}|$ and $|S_{21}|$ at different values of L_{SIW}.

as shown in Fig. 8 (a). When the values of L_{SIW} are changed in the design, the results of RL and IL are not significantly different to that of the simulated and measured values of transition with L_{SIW} = 31 mm (Fig. 8 (b)). This is expectable result, because the transition design formulas (1) and (2) are based on the transition width only and on the assumption that the transition is long enough. Hence, the final length L_{SIW} is 31 mm. The measured minimum and maximum IL are 0.16 and 1.08 dB. This result is including two 6.15 mm length 50-Ohm feeding lines for the probe measurement. It means that the minimum and maximum IL are about 0.0042 and 0.0288 dB/mm for the whole band.

Table I illustrates the performance of the proposed transition and compares it with that of some typical similar transitions available in the literature. One can see that the proposed design functions at the C-band frequency (4.24-8.04 GHz) and has the benefits of easy fabrication (ordinary PCB process), large BW, low IL, and total loss below 25%.

IV. Conclusion

We proposed a broadband transition from CB-CPW to SIW based on the substrate integrated coaxial line. The

TABLE I
COMPARISON OF COMPETITIVE BROADBAND TRANSITION

Ref.	Freq. (GHz)	Structure	RL (dB)	IL (dB)	BW (GHz/%)	Total loss (%)
[14]	8-12	CT-SIW	≥ 15	≤ 0.75	4/48.5	≤ 15
[15]	2.6-3.95	CB-CPW-SIW	≥ 15	≤ 0.2	1.35/36.8	NR
[16]	23.5-40	WG-SIW	≥ 15	≤ 1.2	16.5/52	NR
[17]	48.6-77.3	RWG-SIW	≥ 12	≤ 0.5	28.7/45.5	NR
[13]	4-8	CT-AFSIW	≥ 11	0.55 ± 0.5	8/66	NR
This work	**4.24-8.04** **3.9-4.10***	**SICL-SIW**	≥ 12	**0.16-1.08** **0.18-0.66***	**3.8/63.34** **4.2/70***	≤ 25 $\leq 17*$

(*): Different values of L_{SIW}; **NR**: Not reported

transition is designed and tested in the laboratory. The measured results are well in agreement with the simulation results. For the designed transition, a fractional impedance bandwidth of 63.34% (3.8 GHz of absolute bandwidth) is obtained in measurement. Measured minimum insertion loss of 0.16 dB, and the total loss of less than 25% are obtained. Even though the transition structure is designed, fabricated, and tested in the C-band frequency, the design procedure can be extended to other frequency ranges by proper scaling of the design dimensions with appropriate calculations.

ACKNOWLEDGMENT

The authors would like to acknowledge the financial support by the Science and Engineering Research Board, Govt. of India, in the form of Overseas Visiting Doctoral Fellowship to Anil Kumar Nayak [Award No. SB/S9/Z-16/2016-V (2019-20)]. They would also like to thank Devraj and S. Gaur of Advanced Microwave Lab. of IIT Roorkee for their assistance in the fabrication and measurement of the transition prototypes.

REFERENCES

[1] Z. Kordiboroujeni and J. Bornemann, "New wideband transition from microstrip line to substrate integrated waveguide," *IEEE Trans. Microw. Theory Techn.*, vol. 62, no. 12, pp. 2983–2989, Dec. 2014.

[2] M. Bozzi, A. Georgiadis, and K. Wu, "Review of substrate-integrated waveguide circuits and antennas," *IET Microw. Antennas Propag.*, vol. 5, pp. 909–920, Jun. 2011.

[3] D. Deslandes and K. Wu, "Integrated microstrip and rectangular waveguide in planar form," *IEEE Microw. Compon. Lett.*, vol. 11, no. 2, pp. 68–70, Feb. 2001.

[4] D. Deslandes, "Design equations for tapered microstrip-to-substrate integrated waveguide transitions," in *Proc. IEEE MTT-S Int. Microw. Symp.*, 2010, pp. 704–707.

[5] F. Gatti, M. Bozzi, L. Perregrini, K. Wu, and R. G. Bosisio, "A novel substrate integrated coaxial line (SICL) for wide-band applications," in *Proc. Eur. Microw. Conf.*, 2006, pp. 1614–1617.

[6] S. Mukherjee, P. Chongder, K. V. Srivastava, and A. Biswas, "Design of a broadband coaxial to substrate integrated waveguide (SIW) transition," in *Proc. Asia-Pac. Microw. Conf. (APMC)*, 2013, pp. 896–898.

[7] C. S. Prasad and A. Bishwas, "Effects of coaxial probe dimensions on broadband transition to substrate integrate waveguide," in *Proc. IEEE Appl. Electromagn. Conf. (AEMC)*, 2015, pp. 1–2.

[8] N. Nguyen-Trong, T. Kaufmann, and C. Fumeaux, "Wideband transition from coaxial line to half-mode substrate integrated waveguide," in *Proc. Asia-Pac. Microw. Conf. (APMC)*, 2013, pp. 110–112.

[9] A. Belenguer, A. L. Borja, H. Esteban, and V. E. Boria, "High-performance coplanar waveguide to empty substrate integrated coaxial line transition," *IEEE Trans. Microw. Theory Techn.*, vol. 63, no. 12, pp. 4027–4034, Dec. 2015.

[10] F. Quiles, Á. Belenguer, J. Á. Martínez, V. Nova, H. Esteban, and V. Boria, "Compact microstrip to empty substrate-integrated coaxial line transition," *IEEE Microw. Compon. Lett.*, vol. 28, no. 12, pp. 1080–1082, Dec. 2018.

[11] Y. Shao, X.-C. Li, L.-S. Wu, and J.-F. Mao, "A wideband millimeter-wave substrate integrated coaxial line array for high-speed data transmission," *IEEE Trans. Microw. Theory Techn.*, vol. 65, no. 8, pp. 2789–2800, Aug. 2017.

[12] J. Morro, A. Rodriguez, A. Belenguer, H. Esteban, and V. Boria, "Multilevel transition in empty substrate integrated waveguide," *Electron. Lett.*, vol. 52, no. 18, pp. 1543–1544, 2016.

[13] A.-R. Moznebi, A. Arsanjani, K. Afrooz, and P. Mousavi, "Low-loss and broadband coaxial line to air-filled substrate integrated waveguide transition," *Electron. Lett.*, vol. 55, no. 14, pp. 801–803, 2019.

[14] A. A. Khan and M. K. Mandal, "A compact broadband direct coaxial line to SIW transition," *IEEE Microw. Compon. Lett.*, vol. 26, no. 11, pp. 894–896, Nov. 2016.

[15] R.-Y. Fang, C.-F. Liu, and C.-L. Wang, "Compact and broadband CB-CPW-to-SIW transition using stepped-impedance resonator with 90 deg-bent SLOT," *IEEE Trans. Compon. Packag. Manuf. Technol.*, vol. 3, no. 2, pp. 247–252, Feb. 2013.

[16] I. Mohamed and A. Sebak, "Broadband transition of substrate-integrated waveguide-to-air-filled rectangular waveguide," *IEEE Microw. Compon. Lett.*, vol. 28, no. 11, pp. 966–968, Nov. 2018.

[17] J. Dong, Y. Liu, Z. Yang, H. Peng, and T. Yang, "Broadband millimeter-wave power combiner using compact SIW to waveguide transition," *IEEE Microw. Compon. Lett.*, vol. 25, no. 9, pp. 567–569, Sep. 2015.